Unexpected erosion of chromosome cohesion by a mitotic prophase-like pathway in yeast meiosis

Kiran Challa[1], Miki Shinohara[1, 5], Franz Klein[2], Susan M. Gasser[3] and Akira Shinohara[1] *

[1]Institute for Protein Research, Graduate School of Science, Osaka University, Suita, Osaka 565-0871, Japan
[2]Max F. Perutz Laboratories, University of Vienna, A-1030 Vienna, Austria
[3]Friedrich Miescher Institute for Biomedical Research, 4058 Basel, Switzerland

[5]Present address: Kindai University, School of Agriculture

Running title; meiotic prophase pathway for cohesin release

Keywords; meiosis, cohesin, wapl, PLK, Rec8

*To whom correspondence should be addressed:
Akira Shinohara
Institute for Protein Research, Osaka University,
3-2 Yamadaoka, Suita, Osaka 565-0871 JAPAN
Phone: 81-6-6879-8624
FAX: 81-6-6879-8626
E-mail: ashino@protein.osaka-u.ac.jp

Abstract

In contrast to mitotic division, where cohesion between chromatid arms is dispensable for correct chromosome segregation, arm cohesion distal to crossovers persists in meiosis I. It was therefore assumed that in meiotic prophase chromosome arms retain their full complement of cohesion, thereby preventing chromosome missegregation. Indeed, crossovers that are close to chromosome ends tend to lose distal cohesion and are associated with 5% of missegregation-induced miscarriages. Paradoxically, we found that in budding yeast half of the cohesin complement is released from chromosome arms before the meiotic metaphase/anaphase I transition. This cohesin release is independent of kleisin cleavage and depends on a meiosis-specific phosphorylation of Wpl1 and Rec8 by polo kinase (PLK) and Dbf4-dependent Cdc7 kinase. Cohesin release coincides with a PLK-dependent chromosome compaction in late prophase-I. We predict that a similar process occurs in humans, particularly during the prolonged meiotic prophase I arrest, possibly triggering the high rates of missegregation seen in human oogenesis.

Introduction

Meiosis gives rise to haploid gametes from diploid germ cells. During meiosis, a single round of DNA replication is followed by two consecutive chromosome segregations, meiosis I and II, which reduce the number of chromosomes by half (Marston 2014). Sister chromatid cohesion (SCC) acts as physical connection between the segregating chromosomes and provides resistance to pulling forces by microtubules. SCC at chromosome arms and at kinetochores plays critical roles in chromosome segregation during MI and MII, respectively.

Cohesin mediates SCC and is believed to embrace two sister chromatids in a ring-shaped structure (Gruber et al. 2003). The hetero-dimer of Smc1 and -3 forms a ring, which entraps two DNA molecules. Scc1/Mcd1/Rad21 (hereafter, Scc1 for simplicity) bridges between the Smc1 and Smc3 ATPase head domains to lock the ring. After the loading cohesin during the G1 phase, SCC is established during the S-phase by Eco1-mediated acetylation of Smc3, and is thereafter maintained throughout metaphase. At the anaphase onset, Scc1 is cleaved by the protease separase, which results in the release of the two sister chromatids. Separase activity is inhibited by the protein securin; this process is closely monitored during the spindle-assembly checkpoint (SAC). SAC negatively controls activation of the protein ubiquitination machinery, anaphase-promoting complex/cyclosome (APC/C). APC/C with Cdc20 targets securin for destruction, which enables destruction of cohesin and separation of sister chromatids in anaphase.

Cohesin dynamics are regulated by other cohesin-interacting proteins in yeast and vertebrates, such as Scc3, Pds5 and Rad61/Wpl1 (Wapl) while vertebrates also have a Wapl antagonist sororin. Wapl, together with Pds5, negatively regulates the binding of cohesin to chromatin (Gandhi et al. 2006; Kueng et al. 2006). During late G2 or pro-metaphase in vertebrate cells, cohesin is removed from the majority of chromosome arms via a Scc1-cleavage-independent pathway (Haarhuis et al. 2014). This so-called “prophase pathway” for cohesin removal is mediated by phosphorylation of sororin and Scc3 via polo-like kinase (PLK), and others (Nishiyama et al. 2010; Nishiyama et al. 2013). Phosphorylated sororin is inactive, and can no longer suppress Wapl activity. On the other hand, at the kinetochores, phosphorylation

for the prophase pathway is blocked by the action of the Shugoshin protein, which in turn recruits a phosphatase, PP2A (Marston 2015). PP2A is believed to dephosphoryate proteins involved in the prophase pathway, such as sororin. Interestingly, sororin is not present in lower eukaryotes such as budding yeasts which lacks the prophase pathway in mitosis (Lopez-Serra et al. 2013).

During meiosis, the kleisin subunit, Scc1, is replaced with its meiosis-specific counterpart, Rec8 (and also Rad21L in mammals)(Klein et al. 1999; Ishiguro et al. 2011). Cohesin is a major component of the chromosome axis, which contains two sister chromatids organized into multiple chromatin loops(Klein et al. 1999). During the pachytene stage of prophase-I, homologous chromosomes pair with each other, and synapse along chromosome axes to form a unique meiosis-specific chromosome structure, the synaptonemal complex (SC)(Loidl 2016). The pachytene SC and chromosome axes then dismantle to form a chiasma during diplontene and diakinesis/early metaphase-I. At the onset of anaphase-I, APC/C-Cdc20 induces securin degradation, which activates separase for cleavage of Rec8. Phosphorylation of Rec8 by three kinases, PLK, Dbf4-dependent Cdc7 kinase (DDK), and Casein kinase 1 (CK1) further promotes this cleavage (Brar et al. 2006; Katis et al. 2010). Cleavage of Rec8 is restricted to chromosome arms when Rec8 is protected by Shugoshin at the kinetochores (Kitajima et al. 2004). Whereas it was know that there is a step-wise phosphorylation of Rec8 during meiotic prophase, the role of phosphorylation and cohesin complex dynamics before metaphase I has never been examined. Here we show an unexpected, partial loss of arm cohesion before the metaphase/anaphase I transition, which is independent of cohesin cleavage. This vertebrate “prophase-like” removal of cohesin in meiotic prophase-I is mediated by meiosis-specific phosphorylation of Rec8, as well as phosphorylation of Rad61/Wpl1 by DDK and PLK.

Results

Rec8 shows dynamic relocalization during late prophase-I

Rec8 is a meiosis-specific component of the cohesin complex, and plays an essential role in the establishment of sister chromatid cohesion (SCC). It is also is a major component of chromosome axes, which serve as a platform for various DNA exchanges and chromosome morphogenesis during meiosis (e.g. DNA double-stranded breaks) (Klein et al. 1999). Chromosome axes are dismantled and remodeled during late prophase I. As the late-prophase I stage is very short-lived in the budding yeast, we arrested yeast cells prior to the onset of anaphase I using a meiosis-specific depletion mutant of *CDC20* to examine localization of axis proteins; *CDC20* encodes for the activator of anaphase promoting complex/cyclosome (APC/C). Analysis was conducted on the localization of chromosome proteins in *CDC20mn* (meiotic null) mutants (Lee and Amon 2003) at different times during meiosis. Staining of a central region component of the synaptonemal complex (SC), Zip1 (Sym et al. 1993), allowed us to classify stages of prophase-I. Zip1 staining was classified into three categories: I, dotty staining; II, short-line staining; III, long-line staining. Category III corresponds to the pachytene stage, during which chromosome synapsis occurs. Following pachytene, SC dismantles, resulting in the re-appearance of dotty Zip1 staining (class-I), some of which often co-localize with kinetochores (see below and (Gladstone et al. 2009)). Disassembly of Zip1 was also found to correlate with dissociation of chromosome axis proteins such as Red1 (*Figure 1*)(Rockmill and Roeder 1988). We observed linear Zip1 staining peaks at 5 h in *CDC20mn* mutants, followed by the appearance of Zip1 dots after 6 h (*Figure 1A, B*). When localization of Rec8 was analyzed in pachytene, Rec8 shows linear staining co-localizing with Zip1-lines (*Figure 1A*). Following the pachytene stage, chromosome spreads with Zip1 dots (i.e. at 6 h) started to exhibit dotty Rec8 staining. This indicated that remodeling of cohesin localization takes place at or after SC disassembly. Dotty Rec8 staining in the *CDC20mn* mutants accumulated for up to 8 h, with a final staining intensity of 53±10.8%. The appearance of dotty Rec8 staining occurred concomitantly with disassembly of SCs into Zip1-dots (*Figure 1B*). To further characterize the disassembly status of

the axes, we also examined Rec8-Red1 co-localization at later time points; chromosomal Red1 signals are diminished when Rec8 dots are formed (*Figure 1A, B*). This result further confirmed that Rec8 remodeling occurs at or after disassembly of chromosome axes.

We then used super-resolution microscopy to analyze Rec8-cohesin localization on meiotic chromosomes at high resolution. A structural illuminated microscope (SIM) was used to determine Rec8 localization in *CDC20mn* and *ndt80*, which arrests at the pachytene stage (Xu et al. 1995), mutants (*Figure 1C*). At 5 h, both strains showed two parallel lines of Rec8, which corresponded to two axes of full length SCs (*Figure 1C*). More importantly, the two Rec8 lines do not show a uniform staining, but rather a beads-on-string-like staining was observed, which suggested differential localization of Rec8-cohesin along the chromosome axes. Kinetochore visualization by staining of Ctf19, a centromere protein, revealed that each SC showed a single focus of Ctf19, indicating tight fusion of all four sister kinetochores within the two homologs. Two Rec8 lines were fused around the Ctf19 focal point, suggesting a differential axis structure at peri-centromeric regions with respect to Rec8-cohesin localization. In the *ndt80* mutant, these two Rec8 lines are maintained at times later than 6 h. On the other hand, differential staining patterns were observed between 5 h and 8 h in *CDC20mn* mutants; the two clear parallel lines visible at 5 h disappear at 8h, where discrete foci or short-line staining of Rec8 dominate. This is consistent with our observations by conventional fluorescent microscopy described above. At later time points in *CDC20mn* mutants, a Ctf9 focus at kinetochores is often sandwiched between two separate Rec8 signals on spreads in *CDC20mn* mutants, likely corresponding to the two homologous centromere pairs (*Figure 1C*, see inset).

A previous study reported that signal intensity of Rec8 was diminished during late prophase-I in *CDC20mn* cells (Yu and Koshland 2005). However, they did not observe dotty Rec8 staining at late stages, rather, uniform staining with reduced intensity was seen. This may be due to differences in the antibodies used. In the previous study, localization of HA-tagged Rec8 was examined using an anti-HA antibody; in this study, localization of non-tagged Rec8 was examined using an anti-Rec8 antibody. We also quantified Rec8

signals on chromosomal spreads, and found reduced Rec8 signal at 8 h (61.9±7.6%) as compared with that at 5 h in *CDC20mn* mutants (*Figure 1D*). This was supported by quantification of Rec8 signal in our SIM images (data not shown). Our results strongly suggested that Rec8, and likely as part of the meiotic cohesin complex, dissociates from chromosomes during late prophase-I. Given that decreased Rec8 intensity in cells arrested at meta/anaphase transition was observed during *CDC20* depletion, dissociation of Rec8 from the chromosome seemed to be independent of separase-mediated cleavage.

The localization of a Rec8 mutant protein, Rec8-N, which is resistant to cleavage by separase, was also investigated (Buonomo et al. 2000). The *REC8-N* mutant strain showed normal prophase I progression, but completely blocks metaphase/anaphase-I transition due to Rec8-N's immunity to separase (Buonomo et al. 2000). Similar to the *CDC20mn* mutant, at late prophase-I (e.g. 8 h), *REC8-N* mutant exhibited dotty Rec8 staining with reduced intensity (60±15.7%), while linear staining was observed at 5 h (*Figure 1E*). Previously studies reported that the separase-deficient mutant, *esp1-1*, also shows a decrease in Rec8 intensity at late prophase-I, but these mutants are sick, due to their mitotic defects (Yu and Koshland 2005). Together, all observations supported the hypothesis that remodeling of Rec8 localization at late prophase-I is independent of Rec8 cleavage.

Rec8 dissociates from meiotic chromosomes at late prophase-I

To check whether Rec8-cohesin is indeed released from meiotic chromosomes in *CDC20mn* mutants, we fractionated cell/nuclear lysates to separate the chromatin insoluble and soluble fractions. Chromatin insoluble fractions contained chromosomes with tightly-bound proteins such as histone. At 5 h, most of full-length Rec8 proteins were recovered in the insoluble fraction containing histone H3 in both *ndt80* and *CDC20mn* mutants (*Figure 2A*), as expected. This was consistent with Rec8, and thus cohesin complex, being tightly bound to DNAs and/or chromatin. Rec8 is also chromatin-bound at 8 h in *ndt80* cells. On the other hand, a large proportion of Rec8 protein (69±18.9%) was recovered in soluble fractions at 8 h in the *CDC20mn* mutant; the remaining Rec8 proteins were contained in the insoluble fraction (*Figure 2A, B*).

Interestingly, Rec8 mobility on the gel was much slower in the soluble fraction as compared with that in insoluble Rec8. It has been shown that slow-migrating Rec8 is highly phosphorylated (Brar et al. 2006; Katis et al. 2010). Rec8 is phosphorylated by Dbf4-dependent Cdc7 kinase (DDK), Polo-like kinase (Cdc5), and casein kinase 1 (Hrr25); its phosphorylation is believed to promote Rec8 cleavage by the separase, Esp1 (Brar et al. 2006; Katis et al. 2010). Our results suggested that, alternatively or in addition, a form of Rec8 phosphorylation triggers cohesin dissociation at late prophase-I.

We also checked the status of Smc3 acetylation at K112 and K113 during meiosis via chromatin fractionation (Chan et al. 2012). Acetylation of Smc3 occurs during DNA replication in order to facilitate the establishment of SCC. In *CDC20mn* mutants, most of acetylated Smc3 were found in chromatin-bound fractions at 5 h. This further confirmed our hypothesis that SCC formation is mediated by Smc3 acetylation in prophase-I. At 8 h, 51.6% of acetylated Smc3 was recovered in unbound fractions (*Figure 2A*). This showed that not only Rec8, but also Smc3, a core component of the cohesion complex, is released from the chromatin. Furthermore, acetylated Smc3 was also released in late prophase-I.

To test separase sensitivity of chromatin-bound Rec8 during late prophase-I in *CDC20mn* mutants, we artificially induced expression of the separase, Esp1, in prophase-I under Cdc20 depletion conditions. Esp1 expression is driven by the *CUP1* promoter and copper was added at 5 h for the Esp1 induction (Yoon et al. 2016). Similar to previous results, Rec8 demonstrated punctate staining in chromatins at 8 h in controls. Following Esp1 induction, a large number of Rec8 foci/lines disappeared, leaving only several Rec8 foci on chromosomes (*Figure 2D*). Indeed, signal intensity of Rec8 was reduced to 17.7±6.7% with the induction compared to that at 5 h while without the induction the reduction of Rec8 signal was 50.0±21.7% without Esp1 induction (*Figure 2E*). This demonstrated that most of Rec8 on chromatin during late prophase-I in *CDC20mn* cells are sensitive to separase. This was confirmed by chromatin fractionation (Fig. 2F,G). After 3 h of separase induction, the amount of full length Rec8 on chromatin was reduced to 26.2±10.8% (versus approximately 47.1±16.2% without induction) with the appearance of cleaved Rec8 products. Separase-resistant Rec8 foci often co-localize with the

centromere marker Ctf19 (*Figure 2D*). This confirms that kinetochores already at late-prophase-I are able to protect Rec8 cohesin, from cleavage by separase while arm-bound Rec8 is likely sensitive.

Taken together, the above results showed that Rec8-cohesin dissociates from meiotic chromosomes during late-prophase-I independent of separase activation, suggesting the presence of a cleavage-independent pathway for cohesin release. This is very similar to cohesin release in mammalian (vertebrate) pro-metaphase, where this pathway is called “prophase pathway” (reviewed in (Haarhuis et al. 2014).

Rec8 phosphorylation is required for efficient dissociation of Rec8 at late prophase-I

The requirement for Ndt80 for Rec8 release in the chromatin fractionation (*Figure 2A*) elucidated the role of Rec8 phosphorylation in cohesin release during late prophase-I. We therefore investigated the localization of phosphorylation-deficient Rec8 mutant proteins, Rec8-17A and -29A (Brar et al. 2006; Brar et al. 2009). We introduced *rec8-7A* and *-29* mutations under the *CDC20mn* background, and determined the localization of the resulting Rec8 protein. Phosphorylated Rec8-7A exhibited a band shift, while phosphorylated Rec8-29A displayed little band shift (*Supplemental Figure S2B*). Rec8 staining was defined as linear or dotty staining, which corresponded to the pachytene stage and late (early) prophase-I, respectively. Both Rec8-17A and -29A proteins localized on meiotic chromosomes as linear staining, similar to wild-type proteins (*Figure 3A*; *Supplemental Figure S2C*). In *rec8-17A* mutants, the appearance of dotty Rec8 staining at late time points was slightly delayed as compared with that in the control (*Supplemental Figure S2D*). *Rec8-29A* mutants showed a strong delay in the appearance of dotty Rec8 staining, and consequently the dissociation of cohesin (*Figure 3B*); this was confirmed via intensity measurements (*Figure 3C*). The *rec8-29A* mutant retained 78±25% of its Rec8 signal at 12 h when compared with that at 6 h. However, it is possible that the significant delay in progression to prophase I may be due to defects in the processing of meiotic recombination intermediates in mutants (Brar et al. 2009). Therefore, we also determined localization of Rec8-29A mutant proteins

in chromosome spreads that lacked Red1 signals, which corresponded to late prophase-I (*Figure 1A and 3D*). We found that 67.4% of Red1-negative nuclei showed linear Rec8 expression, which was rare in wild types, indicating a delay of the Rec8 disassembly relative to axis disassembly in the mutant (*Figure 3D, E*). A similar of Rec8 disassembly was also seen relative to Zip1 disassembly in the *rec8-29A* mutant (*Figure 3F, G*). It is likely that Rec8 phosphorylation may promote the dissociation of Rec8 in late prophase-I.

Cdc5 is essential for cleavage-independent Rec8 dissociation from meiotic chromosomes

Given the analogy of Rec8 release in late meiotic prophase-I in yeast with that in mitotic prophase for cohesin release in vertebrates in which Polo-like kinase (PLK) plays a critical role (Haarhuis et al. 2014). We wondered whether Cdc5, a budding yeast PLK, also regulates this dissociation through phosphorylation of Rec8. Indeed, a previous report suggested a role for Cdc5 in Rec8 localization during late prophase-I (Yu and Koshland 2005). We depleted Cdc5 during meiosis in the absence of Cdc20 (*CDC5mn CDC20mn)*. Indeed, Cdc5 depletion greatly reduced the appearance of dotty Rec8 staining, and preserved Rec8 intensity at later time points, such as at 8 h (*Figure 4C-E*); this was supported by chromatin fractionation results (*Figure 4A, B*). At 8 h, approximately half of Rec8 was released from chromatin in *CDC20mn* cells. This release was not seen at 8 h in *CDC5mn CDC20mn* mutants (80±16% at 8 h relative to 5 h). Therefore, Cdc5/PLK is critical for cleavage-independent removal of Rec8 in late prophase-I, possibly through phosphorylation of Rec8. Consistent with this hypothesis, Cdc5 expression was induced after Ndt80 expression at the end of pachytene (Clyne et al. 2003).

To characterize the phospho-status of Rec8 during late prophase-I, we used two phospho-specific antibodies; anti-Rec8-pS179 (PLK site) and anti-Rec8-pS521 (DDK site; kindly provided to us by A. Amon, MIT; (Brar et al. 2006; Attner et al. 2013). Probing chromatin fractions revealed that Rec8-pS179-specific signals were present only at 8 h, but not at 5 h in whole cell lysates from the *CDC20mn,* and the signals were barely detectable in *CDC5mn CDC20mn* mutants, illustrating dependence on Cdc5 (*Figure 4A*). Importantly, at

8 h, the Rec8-pS179 signal was predominantly recovered in chromatin-soluble fractions relative to that in insoluble fractions in *CDC20mn* cells. This indicated that Cdc5-dependent S179 phosphorylation is associated with Rec8 release from meiotic chromatin.

We stained meiotic chromosome spreads with anti-Rec8-pS521 antibody (*Figure 4E*)(Brar et al. 2006), and similar to Rec8 staining results, Rec8-pS521 is linear at 5 h in the *CDC20mn*. However, unlike Rec8, some of Rec8-pS521 foci are brighter than other foci or lines, suggesting local enhancement of S521 phosphorylation by DDK. Importantly, Rec8-pS521-specific signal on spreads was reduced at 8 h, leaving several bright foci. Again, this loss of the signal depends on Cdc5 since *CDC5mn CDC20mn* maintained high levels of Rec8-pS521 signal on chromosomes at late time points (*Figure 4F, G*). Moreover, quantification revealed that Rec8-pS521-specific signal was even stronger reduced compared to Rec8 signals (28.9±20% versus 56.8±18.6%). This is consistent with a model where DDK triggers or contributes to cohesin release in the absence of cleavage.

A previous study showed that ectopic expression of Cdc5 is sufficient for exit from the mid-pachytene stage in *ndt80* mutants; this is triggered by resolution of recombination intermediates into products, as well as the disassembly of SC (without entry into meiosis I) (Clyne et al. 2003). Here we ask whether Cdc5 is sufficient for Rec8 chromatin dissociation by expressing Cdc5 ectopically during an *ndt80Δ* arrest. Expression of Cdc5 was induced by the addition of estradiol into the *CDC5-in ndt80* strain (*Supplemental Figure S4A*). In concert with Zip1-disassembly, Cdc5 induction led to the formation of a punctate Rec8 staining and cohesin release (*Figure 4H, I*). This process was dependent on the kinase activity of Cdc5, as kinase-deprived *CDC5kd* (*CDC5-N209A*; kinase-dead) mutants did not induce remodeling of the Rec8-containing structure during pachytene. This confirmed that Cdc5 is sufficient for cohesion release in mid-pachytene.

Rad61/Wpl1, the Wapl ortholog in yeast, plays a role in cohesin release during late-prophase-I

In the budding yeast, cohesin association in the mitotic G1 phase is inhibited by

a Wapl ortholog, Rad61/Wpl1 (Lopez-Serra et al. 2013); the anti-cohesin activity of Rad61/Wpl1 is counteracted by Eco1-dependent acetylation of Smc3 (Rowland et al. 2009; Sutani et al. 2009) and no prophase-like activity has been reported in G2 phase in yeast mitosis (Lopez-Serra et al. 2013). In mammalian cells, on the other hand, a vertebrate-specific protein, sororin, counteracts Wapl activity (Nishiyama et al. 2010). The fact that the budding yeast does not possess a sororin ortholog prompted us to examine the role of Rad61/Wpl1 in cohesin release during meiosis. Indeed, our previous report showed that in the *rad61/wpl1* mutant, the disassembly of Rec8 is much slower than the other axis component, Red1, whose disassembly is tightly correlated with Rec8 in wild-type (*Figure 1*)(Challa et al. 2016). This suggested that uncoupling in disassembly occurs between the two axis components during late prophase-I in *rad61/wpl1* deletion cells. Localization of Rec8 was examined in *CDC20mn* mutants with deleted Rad61/Wpl1 (e.g. *Figure 5F*). As compared with that in *CDC20mn*, *rad61/wpl1 CDC20mn* cells prolonged the persistence of Rec8 lines to very late time points. Even at 14 h, 32.1±3% *rad61/wpl1* cells contain full linear Rec8 staining (*Figure 5H*). Indeed, signal intensity of Rec8 was unchanged between 5 and 8 h in the absence of Rad61/Wpl1 (*Figure 5G*). This suggests a key role of Rad61/Wpl1 in cohesin release in G2 phase of meiosis. Since Rad61/Wpl1 does not affect cohesin dynamics during the G2 phase of mitosis, it was hypothesized that the role of Rad61 is meiosis-specific. Since Wapl cooperates with Pds5 to antagonize this (Marston 2014), we also examined the effect of meiosis-specific Pds5 depletion on cohesin dynamics. Previously the *PDS5-mn* mutant was observed to show hyper-condensation of chromosomes with formation of SC between sisters (Jin et al. 2009). We confirmed the hyper-condensed SCs in the *PDS5-mn* mutant and found that Rec8 is not degraded in *PDS5-mn CDC20mn* mutant (*Supplemental Figure S3)*. This suggests that Pds5 may work together with Rad61 in the meiotic prophase-like pathway.

We investigated the expression of Rad61-Flag during meiosis by western blot, and found that Rad61 exhibits multiple band shifts on the gel during meiosis (*Figure 5A*). Similar to Rec8, Rad61 expression disappears after 8 h. In addition to the two bands observed during pre-sporulation at 0 h, at least two major meiosis-specific forms of Rad61 were observed; one started to appear at 3 h,

and the other appeared at 5 h. The slowly migrating forms of Rad61 disappear at 8 h leaving a strongly reduced level of the protein relative to early time points. The appearance of two meiotic-species of Rad61 protein as well as its disappearance resembles Rec8, which also shows two major phosphorylated species in addition to the unmodified one (Brar et al. 2006; Katis et al. 2010). It seemed likely that Rad61 bandshifts were due to phosphorylation, and since Rec8 phosphorylation is catalyzed by three kinases, DDK, PLK, and CK1 (Brar et al. 2006; Katis et al. 2010), we checked the effects of these kinases on Rad61 modification. When the kinase activity of analog-sensitive Cdc7 (Cdc7-as) was suppressed by its inhibitor, PP1, band shifts of both Rec8 and Rad61 were greatly diminished in meiosis (*Figure 5B*). We also checked depletion of Cdc5 and found that the second band shifts of both Rad61 and Rec8 at late time points such as 5 and 6 h were nearly abolished in the *CDC5-mn* cells. These results showed that like Rec8, the Rad61-band shift requires both DDK and PLK activities. Rad61 phosphorylation is independent of meiotic recombination such as DSB formation, since *spo11-Y135F* mutants displayed normal Rad61 and Rec8 band shifts (*Supplemental Figure S4B*). On the other hand, Rec8 is essential for the Cdc5-dependent secondary band shift of Rad61, although not the DDK-dependent one (*Figure 5D*). This is consistent with the fact that Rec8 directly binds to Cdc5 kinase (Katis et al. 2010), even though an indirect effect from the derailed meiotic progression in *rec8Δ* cells.

Based on the sequence information of Rad61 (Montagnoli et al. 2006), we mapped putative DDK sites in the N-terminal non-conserved region of Rad61, which is outside of a conserved WAPL domain (*Supplemental Figure S1A*); these sites were as follows: T13, S25, S69, S70, T95, S96, and S97. Various substitution combinations were generated for these putative sites: *rad61-T13A, S25A-FLAG*, *rad61-S69A, S70A-FLAG*, *rad61-T95A, S96A, S97A-FLAG*, *rad61-T13A, S25A, T95A, S69A, S70A, S96A, and S97A-FLAG* (hereafter, *rad61-7A*) and found that meiosis-specific band shifts of Rad61 were compromised in the *rad61-S69A, S70A-FLAG* and *rad61-7A* mutant cells but not in the *rad61-T13A, S25A-FLAG* and *rad61-T95A, S96A, S97A-FLAG* (*Supplemental Figure 4C*). We raised an antibody against a Rad61 peptide containing phospho-S69 and phospho-S70 (*Figure 5D*). Western blotting using

Rad61 phospho-specific antibody clearly revealed two meiosis-specific bands, which were absent in mitosis (*Figure 5D*).

The *rad61-7A* mutant exhibited comparable spore viability as wild-type cells, and entry into meiosis I showed only an hour delay (*Supplemental Fig. S5*), suggesting that Rad61 phosphorylation plays a minor role in early prophase-I. We investigated the effect of *rad61-7A* mutation on Rec8 dissociation at late prophase-I in the absence of Cdc20. Compared to the *CDC20mn* mutant, the *rad61-7A CDC20mn* mutant shows a delayed disappearance of linear straining and appearance of dotty Rec8 staining at late times (*Figure 5F, H*). Again, linear Rec8 expression was frequently detected in Red1-negative nuclei of *rad61-7A CDC20mn* cells (*Figure 5F*). The defective Rec8 release in *rad61-7A* mutants was also confirmed by Rec8-intensity measurements (*Figure 5G*).

This defect of the *rad61-7A* resembles the *rec8-29A* mutant, although it is less pronounced than the *rad61* null mutant. The *rad61-7A rec8-29A* double mutant was more delayed for the disappearance of Rec8 lines in the *CDC20mn* background than in the two single mutants (*Figure 5F*) indicating that both Rec8 and Rad61 phosphorylation contribute to Rec8 release in late prophase-I. The *rad61-7A* and the *rec8-29A* single mutant show 94% and 72.7% spore viability, respectively, while spore viability in the *rad61-7A rec8-29A* double mutant was reduced to 64.1% (*Supplemental Figure S5*).

PLK promotes chromosome compaction in late prophase-I

To observe the consequences of Rec8-cohesin release in late prophase-I, we measured chromosome compaction using two fluorescently marked chromosome loci on chromosome IV in three strains, *ndt80*, *CDC20mn*, and *CDC5mn CDC20mn* (*Figure 6A*). At 0 h, the distance between the two loci was 1.55±0.42 μm in *CDC20mn* mutants, which was reduced to 1.28±0.41 μm at 5 h (Fig.6B) with no further decrease at 8 h in *ndt80* mutants (1.26+/-0.45 [5 h] and 1.22+/-0.39 μm [8 h]), and was consistent with compaction of pachytene chromosomes (Challa et al. 2016). The *CDC20mn* showed an additional decrease of the distance down to 0.58+/-0.27 μm at 8 h of 37% compaction. This indicates specific chromosome compaction (~3-fold) in prophase-I after pachytene. Importantly, this drastic chromosome compaction completely

depends on Cdc5 PLK. *CDC5mn CDC20mn* cells showed only mild compaction of chromosomes both at 5 and 8 h (*Figure 6A, B*).

Discussion

Accordingly, the key message in the headline should not be its regulation, but our results described above suggest the existence of a third step in the release of cohesion in meiotic yeast cells, in addition to the two steps, described (*Figure 7*) (Klein et al. 1999; Buonomo et al. 2000). Prior to the final, cleavage-dependent removal of cohesin, we found cleavage independent removal leaving the meiotic kleisin subunit, Rec8, intact, at late prophase-I, which we call “meiotic prophase pathway” in analogy to the “prophase” pathway in mitotic G2-phase and pro-metaphase of vertebrate cells (Haarhuis et al. 2014). However, mitotic cells in budding yeasts seem to lack the prophase pathway (Lopez-Serra et al. 2013). This is consistent with the fact that budding yeast does not possess a sororin ortholog, which is a key regulator of cleavage-independent removal of cohesin during the late G2 phase in vertebrates (Nishiyama et al. 2010). In contrast to the vertebrate, inactivation of the Wapl inhibitor sororin in mitotic prophase, meiotic yeast cells likely increase the activity of Wapl and Rec8’s affinity for Smc3 by meiosis-specific phosphorylation of Rec8.

Meiotic prophase pathway shares similar mechanism with the vertebrate prophase pathway

Similar to the vertebrate prophase pathway (Haarhuis et al. 2014), the meiotic prophase pathway for cohesin release in the budding yeast meiosi is independent of cohesin cleavage. Rec8 released from meiotic chromosomes was observed in the absence of separase activity in Cdc20-depleted cells as well as in cleavage-resistant *Rec8-N* cells. Moreover, we were able to recover the full-length Rec8 protein, which was stably bound to the chromatin during mid-pachytene, and in chromatin-soluble factions during late prophase-I (*Figure 2*). The above results show that a mechanism releasing Rec8-cohesin independent of cleavage exists.

Like the mammalian prophase pathway, the meiotic prophase pathway

requires WAPL (Rad61/Wpl1) and PLK (Cdc5). During the mitotic G1 phase in yeasts, Rad61/Wpl1 is released from the chromatin, and is known to promote the dynamic binding of mitotic cohesin (Lopez-Serra et al. 2013). During the mammalian mitotic prophase and the yeast G1 phase, the Wapl-Pds5 a interaction mediates the opening of the exit gate between Scc1-Smc3 (Chan et al. 2012). Judged by the role of Rad61, the meiotic prophase pathway is mechanistically similar to the mammalian prophase pathway and the G1 pathway in yeast; the release of meiotic cohesin in late prophase-I may occur through the opening at the interface between Rec8 and Smc3 (*Figure 7, bottom*). It might be possible to confirm this with a Smc3-Rec8 fusion protein that locks the interface between the meiotic kleisin, Rec8, and Smc3. The fact that acetylated Smc3 and full-length Rec8 were recovered in chromatin-unbound fractions during late prophase-I indicated that the Rec8-cohesin complex promoted SCC through Eco1-dependent acetylation before its release from meiotic chromosomes.

Yeast meiotic prophase pathway is different from the mammalian prophase pathway

In vertebrate cells, sororin inactivation is essential for the cleavage-independent release of cohesin. Sororin is likely bound to the Scc1/Rad21 domain, to which Wapl also binds. Sororin binding induces steric hindrance to the binding surface of Scc1, and as a result, Wapl is unable to open the exit gate (Marston 2014). Phosphorylated sororin dissociates from cohesion, allowing for binding between Wapl and Scc1, which leads to opening of the gate. However, the budding yeast lacks a sororin ortholog. During yeast mitosis, anti-cohesin activity of Rad61/Wpl1 is counteracted by Eco1-mediated acetylation of Smc3. Thus, Smc3-acetylation is sufficient to antagonize Rad61 activity in the yeast (Rowland et al. 2009; Sutani et al. 2009). Smc3 acetylation is maintained during prophase-I of meiosis (this paper). Rather than inactivating a negative regulator for Wpl, meiotic cells seem to display a novel mechanism for cohesin release through enhancement of Rad61/Wpl1 activity.

We identified two critical regulators of the meiosis prophase pathway, Rad61 (and Pds5) and Cdc5, both of which are expressed during mitosis and

meiosis. Nevertheless, our study results show a meiosis-specific regulation of cohesin removal. Since during meiosis, Scc1 is replaced with the meiosis-specific Rec8; Rec8 is a key determinant for meiosis-specific prophase pathway. Indeed, we showed that Rec8 phosphorylation is required for cohesin release in late prophase-I. Thus, meiosis-specificity is conferred by the Rec8 kleisin. In addition, Rad61 is phosphorylated only in meiotic prophase-I by the two mitotic kinases, DDK and PLK. Rec8 is known to interact directly with PLK and Cdc5 (Katis et al. 2010). Consistent with this, we show here that the meiosis-specific Cdc5-dependent phosphorylation of Rad61 requires Rec8. Therefore, Rec8 has dual functions in cohesin release during meiosis. Rec8 exhibits intrinsic properties to respond to anti-cohesin activity of Wapl, as well as the ability to enhance Wapl activity through promoting its phosphorylation The exact mechanisms that induce meiosis-specific DDK-dependent phosphorylation is induced in early prophase-I is unknown. We know that Rec8 at least does not play an essential role in this phosphorylation, as *rec8* mutants were able to initiate meiosis-specific DDK-dependent phosphorylation of Rad61. We propose that phosphorylation of Rad61 may augment anti-cohesin activities, and consequently, the gate-opening activity of the protein. Thus, we propose that Rec8 phosphorylation may loosen the binding of Rec8 to Smc3 and Rad61 to unlock the Rec8-Smc3 gate, which is closed by the acetylation of Smc3.

The meiotic prophase pathway is conserved in higher eukaryotes

The cleavage-independent pathway of cohesin release during meiosis is conserved in higher eukaryotes such as nematodes, plants, and mammals. In these organisms, differential distributions of reduced cohesin signals on chromosomes or chromosome arms were observed in late prophase-I, as in diakinesis. In nematodes, cohesin on short arms, but not on long arms, is likely to be removed, in a manner dependent on aurora kinase, *air-2* (Rogers et al. 2002). Interestingly, in nematodes, Wapl, which is encoded by *wapl-1*, controls the dynamics of kleisin COH3/4-containing cohesion, but not of cohesin associated with Rec8 (Crawley et al. 2016). In *Arabidopsis thaliana*, most Rec8 molecules, and by association, cohesins, are released from meiotic chromosomes during the diplotene stage, and this is mediated by Wapl (De et al.

2014). Like yeast, *C. elegans* and *A. thaliana* lack a clear sororin ortholog.

In mouse spermatocytes, the Rad21L kleisin, but not Rec8, is predominantly removed during the diplotene stage. Interestingly, this removal is partially dependent on PLK (Ishiguro et al. 2011). Recently, a novel regulatory circuit for cohesin removal was described during spermatogenesis, where Nek1 kinase-dependent "de"phosphorylation of Wapl promotes its retention on chromosomes and consequently the release of of cohesin (Brieno-Enriquez et al. 2016). It was observed that during meiosis in mouse spermatocytes, phosphorylation of Wapl inhibits its activity. This is in sharp contrast to the role of Rad61 phosphorylation in the budding yeast. This may again correlate with the absence of sororin from yeast.

Local regulation of protection and promotion of cohesin removal along the chromosomes

Results presented in this work showed that during Cdc20-depletion, approximately 50-60% of chromosome-bound Rec8 at the pachytene stage can be dissociated from chromosomes during late prophase-I. On the other hand, 40-50% of Rec8 remains stably bound to chromosomes during late prophase I, suggesting that these Rec8 molecules are either protected against or are not activated by the meiotic prophase pathway. Most of the chromatin-bound Rec8 at late prophase-I is still sensitive to artificially expressed separase while, as expected, Rec8 at kinetochores is resistant to it. At the onset of anaphase-I, kinetochore-bound Rec8 is protected by a molecule called Shugoshin (Sgo1)(Kitajima et al. 2006; Katis et al. 2010), which is bound to kinetochores during late prophase-I. Indeed, artificial expression of separase in pachytene-arrested cells; e.g. *ndt80* mutant, completely removes Rec8 even at kinetochores (Yoon et al. 2016). These studies suggested that full protection of kinetochore-bound Rec8 is established only after the exit of pachytene. In the mammalian prophase pathway, kinetochore-bound cohesin is protected by Shugoshin/PP2A via dephosphorylating subunits such as sororin. A similar protection mechanism seen in the mammalian mitotic prophase pathway may also operate on cohesins that are bound to meiotic chromosome arms and to the kinetochores. However, these two protection of arm cohesin, which is sensitive

to separase must be functionally distinct from CEN-cohesion, which is not.

The meiotic prophase pathway requires DDK- and PLK-dependent meiosis-specific phosphorylation of Rec8 and Rad61. Indeed, we showed that Rec8 released from chromosomes is more phosphorylated than the complement that remains tightly bound to chromosomes. One plausible mechanism for the observed protection against the prophase pathway is local activation of dephosphorylated cohesin, as seen at kinetochores, where Shugoshin recruits the phosphatase PP2A. This is similar to the role that Sgo1 plays in protection of centromeric cohesin at the onset of anaphase-I in vertebrate meiosis.

Alternatively, local activation by phosphorylation of Rec8 and Rad61 may be a mechanism that promotes cohesin release in distinct chromosomal regions. For instance, local removal of cohesin at the site of chiasmata (Kleckner 2006) may be a necessary step in the formation of normal diplotene bivalents. Further studies are required, to see if Wpl is be involved in this.

Is Rec8 phosphorylation indeed required for the cleavage by separase?

Previous reports strongly suggested that phosphorylation of Rec8 by DDK, PLK, and CK1 is essential for cleavage by separase (Brar et al. 2006; Katis et al. 2010). However, this was not directly tested by an *in vitro* cleavage assay. Our results presented here suggest that Rec8 phosphorylation by DDK and PLK is essential for Rec8-cohesin dissociation at late prophase-I. At the centromeres, Shugoshin seems to be able to protect Rec8 from cleavage-independent dissociation via the recruitment of PP2A (Kitajima et al. 2006). The relationship between phosphorylation of cohesin subunits and Shugoshin in meiosis is reminiscent of that in the mammalian mitotic prophase pathway, where Sgo2-PP2A mediates the dephosphorylation of sororin and other molecules to counteract the effect of Wapl. If Rec8 and Rad61 dephosphorylation protects the dissociation of cohesin from chromosomes, chromosome-bound cohesin would become hypo-phosphorylated, which is a poor substrate for separase. In other words, phosphorylation of Rec8 is not an essential prerequisite for cleavage by separase. We and others (Yoon et al. 2016) showed that chromosome-bound Rec8 with reduced phosphorylation could be used as a substrate for separase-mediated cleavage *in vivo*, since ectopic expression of separase in

late prophase-I was sufficient for the removal of Rec8-cohesin from chromosome arms, but not from centromeres. We proposed that phosphorylation of Rec8 is required for cleavage-independent dissociation of cohesin, in contrast to release through the cleavage of Rec8.

Functions of the meiotic prophase pathway

Given that cohesin at the chromosome arm is important for chromosome segregation in MI, one may suggest that the meiotic-prophase pathway is dangerous in meiotic cells. This begs the questions of why meiosis has retained this dangerous pathway through time. In other words, what is the role of cohesin removal in late prophase-I? It is known that during late prophase-I, which corresponds to diplotene and diakinesis in other organisms, drastic changes in chromosome morphology occur (Zickler and Kleckner 1999). This includes strong compaction while chiasmata emerge, to prepare for chromosome segregation. In meiosis I, the chiasmata are essential for chromosome segregation. Indeed, loss of cohesion around chiasmata sites has been observed in various organisms (Kleckner 2006). In worms, Wapl-dependent cohesin removal promotes recombination-mediated change of meiotic chromosome structures (Crawley et al. 2016).

One likely function of cohesin release in late prophase-I is to promote chiasma formation. Individualization of chromosomes may play a role in the proper development of chiasmata. In addition, in late prophase-I, chromosomes show drastic compaction. Even in the budding yeast, late meiotic chromosomes are compacted by approximately 3 fold as compared with their sizes in G1 (Yu and Koshland 2005)(this study). Concomitant with this drastic compaction of chromosomes in late prophase-I, condensin has been shown to bind to meiotic chromosomes following the pachytene stage (Yu and Koshland 2005; Jin et al. 2009). The binding of condensin not only promotes condensation of chromosomes, but also facilitates the release of cohesin (Yu and Koshland 2005). Condensin-dependent chromosome compaction may promote individualization of chromatids. In this work we show that Cdc5 depletion causes both, a failure in the meiotic prophase pathway and a corresponding defect in

chromosome compaction. This is consistent with a role of cohesin removal in compaction, although other interpretations are possible.

It has been proposed that the mitotic prophase pathway controls decatenation of sister chromatids, microtubule attachment, and cohesin turnover (Haarhuis et al. 2014). Similar to vertebrate mitosis, the meiotic prophase pathway also controls DNA decatenation and microtubule attachment (Haarhuis et al. 2014). However, cohesin removal during Rec8-cohesin turnover is unlikely to occur during meiosis, since, after meiosis, spores form, which re-synthesize all cohesin components including the mitotic kleisin Scc1 upon germination. Following germination, all components of cohesion, including the mitotic kleisin Scc1, are re-synthesized; the same is true during mammalian spermatogenesis. On the other hand, the meiotic prophase pathway plays a detrimental role in cohesin turnover in the meiotic dictyate stage in female mammalian oocytes, where cohesion needs to be maintained for decades (Tachibana-Konwalski et al. 2010). This shows, that apparently separase independent cohesin dissociation is such a basic property that it can't be turned off in meiotic prophase to safeguard chromosome segregation. What that basic property is, whether it is cohesin removal to make space for condensin, or local cohesin removal to allow chiasma morphogenesis or another function is a question that remains to be answered in future studies.

Materials and methods

Strains and strain construction

All strains described here are derivatives of SK1 diploid strains, NKY1551 (*MATα/MAT**a**, ho::LYS2/", lys2/", ura3/", leu2::hisG/", his4X-LEU2-URA3/his4B-LEU2, arg4-nsp/arg4-bgl*). Strain genotypes are given in Supplemental Table S1. *CEN4-GFP/TEL4-GFP* and Esp1-overexpression strains was provided by Dr. Doug Koshland and Dr. Keun P. Kim, respectively.

Antisera and antibodies

Anti-Zip1, anti-Red1, and anti-Rec8 antisera for cytology and western blotting have been described previously (Shinohara et al. 2008; Zhu et al. 2011). Secondary antibodies conjugated with Alxea488 and Alexa594 dyes (Molecular Probes, Life Technologies, UK) were used for the detection of the primary antibodies. Anti-Rec8-pS179 (PLK site) and anti-Rec8-pS521 (DDK site) were generous gifts from Dr. Angelika Amon (MIT). Anti-acetyl-Smc3 was a gift by Dr. Katsu Shirahige (U. of Tokyo). Anti-Rad61-PS69 and pS70 antibody was raised in rabbit using a Rad61 peptide containing pS69 and pS70 by a company (MBL Co. Ltd).

Cytology

Immunostaining of chromosome spreads was performed as described previously (Shinohara et al. 2000; Shinohara et al. 2003). Stained samples were observed using an epi-fluorescence microscope (BX51; Olympus, Japan) with a 100X objective (NA1.3). Images were captured by CCD camera (CoolSNAP; Roper, USA), and afterwards processed using IP lab and/or iVision (Sillicon, USA), and Photoshop (Adobe, USA) software tools.

SIM imaging

The structured illumination microscopy in Figure 1C and 1D were carried out using super resolution-structured illumination (SR-SIM) microscope (Elyra S.1 [Zeiss], Plan-Apochromat 63x/1.4 NA objective lens, EM-CCD camera [iXon 885; Andor Technology], and ZEN Blue 2010D software [Zeiss]) at Friedrich

Miescher Institute for Biomedical Research, Switzerland. Image Processing was performed with Zen software [Zeiss], image J and Photoshop.

Fluorescence intensity measurement

Mean fluorescence of the whole nucleus was quantified with Image J. Quantification was performed using unprocessed raw images and identical exposure time setting in DeltaVision system (Applied Precision, USA). The area of a nuclear spread was defined as an oval, and the mean fluorescence intensity was measured within this area.

Chromatin fractionation

Chromatin fractionation was performed as described previously[37]. The cells were digested with Zymolyase 100T (Nakarai Co. Ltd) and the spheroplasts were pelleted. The pellets were resuspended in five volumes of hypotonic buffer (HB; 100 mM MES-NaOH, pH 6.4, 1 mM EDTA, 0.5 mM $MgCl_2$) supplemented with a protease inhibitor cocktail (Sigma, USA). After 5 min, 120 µl of whole cell extract (WCE) were layered onto 120 µl of 20% (W/V) sucrose in HB and centrifuged for 10 min at 16,000 *g*. The supernatants were saved and the pellets were resuspended in 120 µl EBX buffer (50 mM HEPS-NaOH, pH 7.4, 100 mM KCl, 1 mM EDTA, 2.5 mM $MgCl_2$, 0.05% Triton X100) and centrifuged for 10 min at 16,000 *g*. The pellets were again collected and resuspended in EBX buffer with 5 units/ml DNase I and 1 mM $MgCl_2$ for 5 min. The supernatants were saved for further analysis.

Yeast culture

Yeast cell culture and time-course analyses of the events during meiosis and the cell cycle progression were performed as described previously (Shinohara et al. 2003).

Statistics

Means ± S.D values are shown. Datasets were compared using the Mann-Whitney U-test. χ^2-test was used for proportion. Multiple test correction was done with Bonferroni's correction. *, **, *** show P-values of <0.05, <0.01

and <0.001, respectively.

ACKNOWLEDGEMENTS

We are grateful to Drs. A. Marston, K. Matsuzaki, and H. B. D. P. Rao as well as the members of the Shinohara lab for helpful discussions. We thank Dr. A. Seeber and Dr. L. Gelman of the FMI for help with Ms. A. Murakami and H. Wakabayashi for excellent technical assistance. We are grateful to Drs. A. Amon, K. Kim, D. Koshland, K. Shirahige, K. Nasmyth, and W. Zachariae for materials used in this study. This work was supported by JSPS KAKENHI Grant Number; 22125001, 22125002, 15H05973 and 16H04742 to A.S. M.S. was supported by the Japan Society for the Promotion of Science (JSPS) through the Funding Program for Next Generation World-Leading Researchers (NEXT Program).

References

Attner MA, Miller MP, Ee LS, Elkin SK, Amon A. 2013. Polo kinase Cdc5 is a central regulator of meiosis I. *Proc Natl Acad Sci U S A* **110**: 14278-14283.

Brar GA, Hochwagen A, Ee LS, Amon A. 2009. The multiple roles of cohesin in meiotic chromosome morphogenesis and pairing. *Mol Biol Cell* **20**: 1030-1047.

Brar GA, Kiburz BM, Zhang Y, Kim JE, White F, Amon A. 2006. Rec8 phosphorylation and recombination promote the step-wise loss of cohesins in meiosis. *Nature* **441**: 532-536.

Brieno-Enriquez MA, Moak SL, Toledo M, Filter JJ, Gray S, Barbero JL, Cohen PE, Holloway JK. 2016. Cohesin Removal along the Chromosome Arms during the First Meiotic Division Depends on a NEK1-PP1gamma-WAPL Axis in the Mouse. *Cell Rep* **17**: 977-986.

Buonomo SB, Clyne RK, Fuchs J, Loidl J, Uhlmann F, Nasmyth K. 2000. Disjunction of homologous chromosomes in meiosis I depends on proteolytic cleavage of the meiotic cohesin Rec8 by separin. *Cell* **103**: 387-398.

Challa K, Lee MS, Shinohara M, Kim KP, Shinohara A. 2016. Rad61/Wpl1 (Wapl), a cohesin regulator, controls chromosome compaction during meiosis. *Nucleic Acids Res* **44**: 3190-3203.

Chan KL, Roig MB, Hu B, Beckouet F, Metson J, Nasmyth K. 2012. Cohesin's DNA exit gate is distinct from its entrance gate and is regulated by acetylation. *Cell* **150**: 961-974.

Clyne RK, Katis VL, Jessop L, Benjamin KR, Herskowitz I, Lichten M, Nasmyth K. 2003. Polo-like kinase Cdc5 promotes chiasmata formation and cosegregation of sister centromeres at meiosis I. *Nat Cell Biol* **5**: 480-485.

Crawley O, Barroso C, Testori S, Ferrandiz N, Silva N, Castellano-Pozo M, Jaso-Tamame AL, Martinez-Perez E. 2016. Cohesin-interacting protein WAPL-1 regulates meiotic chromosome structure and cohesion by antagonizing specific cohesin complexes. *Elife* **5**: e10851.

De K, Sterle L, Krueger L, Yang X, Makaroff CA. 2014. Arabidopsis thaliana

WAPL is essential for the prophase removal of cohesin during meiosis. *PLoS Genet* **10**: e1004497.

Gandhi R, Gillespie PJ, Hirano T. 2006. Human Wapl is a cohesin-binding protein that promotes sister-chromatid resolution in mitotic prophase. *Curr Biol* **16**: 2406-2417.

Gladstone MN, Obeso D, Chuong H, Dawson DS. 2009. The synaptonemal complex protein Zip1 promotes bi-orientation of centromeres at meiosis I. *PLoS Genet* **5**: e1000771.

Gruber S, Haering CH, Nasmyth K. 2003. Chromosomal cohesin forms a ring. *Cell* **112**: 765-777.

Haarhuis JH, Elbatsh AM, Rowland BD. 2014. Cohesin and its regulation: on the logic of X-shaped chromosomes. *Dev Cell* **31**: 7-18.

Ishiguro K, Kim J, Fujiyama-Nakamura S, Kato S, Watanabe Y. 2011. A new meiosis-specific cohesin complex implicated in the cohesin code for homologous pairing. *EMBO Rep* **12**: 267-275.

Jin H, Guacci V, Yu HG. 2009. Pds5 is required for homologue pairing and inhibits synapsis of sister chromatids during yeast meiosis. *J Cell Biol* **186**: 713-725.

Katis VL, Lipp JJ, Imre R, Bogdanova A, Okaz E, Habermann B, Mechtler K, Nasmyth K, Zachariae W. 2010. Rec8 phosphorylation by casein kinase 1 and Cdc7-Dbf4 kinase regulates cohesin cleavage by separase during meiosis. *Dev Cell* **18**: 397-409.

Kitajima TS, Kawashima SA, Watanabe Y. 2004. The conserved kinetochore protein shugoshin protects centromeric cohesion during meiosis. *Nature* **427**: 510-517.

Kitajima TS, Sakuno T, Ishiguro K, Iemura S, Natsume T, Kawashima SA, Watanabe Y. 2006. Shugoshin collaborates with protein phosphatase 2A to protect cohesin. *Nature* **441**: 46-52.

Kleckner N. 2006. Chiasma formation: chromatin/axis interplay and the role(s) of the synaptonemal complex. *Chromosoma* **115**: 175-194.

Klein F, Mahr P, Galova M, Buonomo SB, Michaelis C, Nairz K, Nasmyth K. 1999. A central role for cohesins in sister chromatid cohesion, formation of axial elements, and recombination during yeast meiosis. *Cell* **98**:

91-103.

Kueng S, Hegemann B, Peters BH, Lipp JJ, Schleiffer A, Mechtler K, Peters JM. 2006. Wapl controls the dynamic association of cohesin with chromatin. *Cell* **127**: 955-967.

Lee BH, Amon A. 2003. Role of Polo-like kinase CDC5 in programming meiosis I chromosome segregation. *Science* **300**: 482-486.

Loidl J. 2016. Conservation and Variability of Meiosis Across the Eukaryotes. *Annu Rev Genet* **50**: 293-316.

Lopez-Serra L, Lengronne A, Borges V, Kelly G, Uhlmann F. 2013. Budding yeast Wapl controls sister chromatid cohesion maintenance and chromosome condensation. *Curr Biol* **23**: 64-69.

Marston AL. 2014. Chromosome segregation in budding yeast: sister chromatid cohesion and related mechanisms. *Genetics* **196**: 31-63.

-. 2015. Shugoshins: tension-sensitive pericentromeric adaptors safeguarding chromosome segregation. *Mol Cell Biol* **35**: 634-648.

Montagnoli A, Valsasina B, Brotherton D, Troiani S, Rainoldi S, Tenca P, Molinari A, Santocanale C. 2006. Identification of Mcm2 phosphorylation sites by S-phase-regulating kinases. *J Biol Chem* **281**: 10281-10290.

Nishiyama T, Ladurner R, Schmitz J, Kreidl E, Schleiffer A, Bhaskara V, Bando M, Shirahige K, Hyman AA, Mechtler K et al. 2010. Sororin mediates sister chromatid cohesion by antagonizing Wapl. *Cell* **143**: 737-749.

Nishiyama T, Sykora MM, Huis in 't Veld PJ, Mechtler K, Peters JM. 2013. Aurora B and Cdk1 mediate Wapl activation and release of acetylated cohesin from chromosomes by phosphorylating Sororin. *Proc Natl Acad Sci U S A* **110**: 13404-13409.

Rockmill B, Roeder GS. 1988. RED1: a yeast gene required for the segregation of chromosomes during the reductional division of meiosis. *Proc Natl Acad Sci U S A* **85**: 6057-6061.

Rogers E, Bishop JD, Waddle JA, Schumacher JM, Lin R. 2002. The aurora kinase AIR-2 functions in the release of chromosome cohesion in Caenorhabditis elegans meiosis. *J Cell Biol* **157**: 219-229.

Rowland BD, Roig MB, Nishino T, Kurze A, Uluocak P, Mishra A, Beckouet F, Underwood P, Metson J, Imre R et al. 2009. Building sister chromatid

cohesion: smc3 acetylation counteracts an antiestablishment activity. *Mol Cell* **33**: 763-774.

Shinohara M, Gasior SL, Bishop DK, Shinohara A. 2000. Tid1/Rdh54 promotes colocalization of rad51 and dmc1 during meiotic recombination. *Proc Natl Acad Sci U S A* **97**: 10814-10819.

Shinohara M, Oh SD, Hunter N, Shinohara A. 2008. Crossover assurance and crossover interference are distinctly regulated by the ZMM proteins during yeast meiosis. *Nat Genet* **40**: 299-309.

Shinohara M, Sakai K, Ogawa T, Shinohara A. 2003. The mitotic DNA damage checkpoint proteins Rad17 and Rad24 are required for repair of double-strand breaks during meiosis in yeast. *Genetics* **164**: 855-865.

Sutani T, Kawaguchi T, Kanno R, Itoh T, Shirahige K. 2009. Budding yeast Wpl1(Rad61)-Pds5 complex counteracts sister chromatid cohesion-establishing reaction. *Curr Biol* **19**: 492-497.

Sym M, Engebrecht JA, Roeder GS. 1993. ZIP1 is a synaptonemal complex protein required for meiotic chromosome synapsis. *Cell* **72**: 365-378.

Tachibana-Konwalski K, Godwin J, van der Weyden L, Champion L, Kudo NR, Adams DJ, Nasmyth K. 2010. Rec8-containing cohesin maintains bivalents without turnover during the growing phase of mouse oocytes. *Genes Dev* **24**: 2505-2516.

Xu L, Ajimura M, Padmore R, Klein C, Kleckner N. 1995. NDT80, a meiosis-specific gene required for exit from pachytene in Saccharomyces cerevisiae. *Mol Cell Biol* **15**: 6572-6581.

Yoon SW, Lee MS, Xaver M, Zhang L, Hong SG, Kong YJ, Cho HR, Kleckner N, Kim KP. 2016. Meiotic prophase roles of Rec8 in crossover recombination and chromosome structure. *Nucleic Acids Res* **44**: 9296-9314.

Yu HG, Koshland D. 2005. Chromosome morphogenesis: condensin-dependent cohesin removal during meiosis. *Cell* **123**: 397-407.

Zhu Z, Mori S, Oshiumi H, Matsuzaki K, Shinohara M, Shinohara A. 2011. Cyclin-dependent kinase promotes formation of the synaptonemal complex in yeast meiosis. *Genes Cells* **15**: 1036-1050.

Zickler D, Kleckner N. 1999. Meiotic chromosomes: integrating structure and function. *Annu Rev Genet* **33**: 603-754.

Figure Legends

Figure 1. Rec8 shows dynamic localization in late meiotic prophase-I

(A) Immunostaining analysis of Rec8 (red) and SC protein Zip1 (green; top) and Rec8 (red) and axis protein Red1 (green; bottom) in *CDC20-mn* (KSY642/643) strain. Representative image with or without DAPI (blue) dye is shown. Rec8 staining in the *CDC20-mn* was classified as linear (5 h) and dotty (8 h) classes. The bar indicates 2 μm.

(B) Kinetics of Rec8 (left), Zip1 (middle) and Red1 (right) staining in *CDC20-mn* (KSY642/643) strain was analyzed. A minimum 100 cells were counted at each time point. Error bars (Rec8) show the standard deviation (S.D.; n=3). Zip1 staining is classified as follows: dotty (blue); short linear (green); full linear staining (red). Red1 staining is classified as follows; dot (light blue); short linear (light purple); full linear staining (purple).

(C) SR-SIM microscopic observation of Rec8 (red) and Ctf19 (green) (left), and Rec8 (red) and Red1 (green) (right), in *CDC20-mn* (KSY642/643) cells and *ndt80* (KSY467/468) cells. Representative image with or without DAPI (blue) dye is shown. White insets are shown in a magnified view at right. The bar indicates 2μm.

(D) Total signal intensity of Rec8, Red1, and DAPI in image shown (A) was measured in *CDC20-mn* (KSY642/643) and *ndt80* (KSY467/468) cells. A minimum 30 nuclei were quantified in representative time points. Error bars show the S.D. (n=3).

(E) Localization of Rec8 (red) in *CDC20-mn* (KSY642/643), *REC8-N* (KSY597) and *ndt80* (KSY467/468) mutants. Quantification of total Rec8 and DAPI signal intensity in these mutants (bottom) were analyzed as shown in (D).

Figure 2. Rec8 dissociates from meiotic chromosomes at late prophase-I

(A) Chromatin fractionation assay was carried out using *CDC20-mn* (KSY642/643) and *ndt80* (KSY467/468) mutant cells. Western blotting was performed for whole cell extracts (W), soluble fractions (S) and chromatin-bound fraction (P). Rec8 (top) and acetyl-Smc3 (second) were

probed together with tubulin (third) and Histone 2B (H2B; bottom) as controls for soluble and chromatin-bound proteins, respectively.

(B) Quantification of Rec8 band intensity in (A) is shown. Rec8-enrichment to chromatin is expressed as a ratio of Rec8 to H2B levels while the soluble fraction of Rec8 is based on the ratio of Rec8 to tubulin levels. Rec8 level in *CDC20-mn* strain whole cell extracts (W) at 5 h was used to normalize the values. Error bars show the S.D. (n=3).

(C) Intensity of acetyl-Smc3 shown in (A) was quantified and analyzed as described in (B).

(D) Single culture of *CDC20-mn pCUP-Esp1-9myc* (KSY1009/1010) strain was synchronized and divided into two cultures; then Esp1 expression was induced by addition of 50 μM $CuSO_4$ at 5 h. Prepared chromosome spreads were immuno-stained for Rec8 (red) and Ctf19 (green). Representative images are shown. The bar indicates 2 μm.

(E) Total Rec8 and DAPI signal intensity was quantified as shown in (C). A minimum 30 nuclei were quantified in each representative time points. Error bars show the S.D. (n=3).

(F) Chromatin fractionation assay of *CDC20-mn pCUP-Esp1-9myc* (KSY1009/1010) cells without and with overexpression of Esp1 was carried out as shown in (A).

(G) Quantification of Rec8 levels in *CDC20-mn pCUP-ESP1-9myc* (KSY1009/1010) strain (E) was analyzed as shown in (B). Whole cell extracts (W) at 5 h sample was used for normalization.

Figure 3. Rec8 phosphorylation is required for efficient dissociation of Rec8 at late prophase-I

(A) Localization of Rec8 (red) and Ctf19 (green) on chromosome spreads was analyzed for *CDC20-mn* (KSY642/643) and *CDC20-mn rec8-29A* (KSY866/867) cells. Representative image with or without DAPI (blue) dye is shown. The bar indicates 2μm.

(B) Kinetics of Rec8 staining classes in (A) was analyzed as in Figure 1B. A minimum 100 cells were analyzed at each time point. Error bars show the S.D. (n=3).

(C) Total Rec8 and DAPI signal intensity in (C) was quantified as described in Figure 1D. Error bars show the S.D. (n=3).

(D) Localization of Rec8 (red) and Red1 (green) spreads was studied in *CDC20-mn* (KSY642/643) and *CDC20-mn rec8-29A* (KSY866/867).

(E) Kinetics of Rec8 (left) and Red1 (right) in (D) was analyzed as in Figure 1D. Rec8 staining in this strain classified as follows: dot (blue); short linear (dark yellow); full linear staining (red) and Red1 staining in this strain classified as follows: dot (light blue); short linear (light purple); full linear staining (purple).

(F) Localization of Rec8 (red) and Zip1 (green) was examined in *CDC20-mn* (KSY642/643) and *CDC20-mn rec8-29A* (KSY866/867) cells.

(G) Kinetics of Zip1 staining in (F) was classified shown as in Figure 1B. Error bars show the variation from two independent experiments.

Figure 4. Cdc5 is essential for cleavage-independent Rec8 dissociation from meiotic chromosomes

(A) Chromatin fractionation assay for *CDC20-mn* (KSY642/643) and *CDC20-mn CDC5-mn* (KSY659/660) mutant cells was carried out as described in Figure 2A.

(B) Quantification of Rec8 bands in chromatin fractionation (A) was analyzed as in Figure 2B. Rec8 level in *CDC20-mn* strain whole cell extracts (W) at 5 h sample was used to normalize to 1. Error bars show the S.D. (n=3).

(C) Localization of Rec8 (red) in *CDC20-mn* (KSY642/643) and *CDC20-mn CDC5-mn* (KSY659/660) mutants. Representative image is shown. The bar indicates 2 μm.

(D) Kinetics of Rec8 in (C) was classified as shown in Figure 1B. Error bars show the S.D. (n=3).

(E) Quantified total Rec8 and DAPI signal intensity in (D) was analyzed as shown in Figure 1D. Error bars show the S.D. (n=3).

(F) Localization of Rec8 (red) and Rec8-pS521 (green) was analyzed in *CDC20-mn* (KSY642/643) *CDC20-mn CDC5-mn* (KSY659/660) cells.

(G) Total Rec8, Rec8-pS521, and DAPI signal intensity in (F) was studied as in Figure 1D. Error bars show the S.D.

(H) Localization of Rec8 (red) in *ndt80* (KSY467/468), *ndt80 GALp-CDC5 GAL4-DB-ER* without estradiol induction (-ER) (KSY887/888), *ndt80 GALp-CDC5-N209A GAL4-DB-ER* with estradiol induction (+ER) (KSY882/883) and *ndt80 GALp-CDC5 GAL4-DB-ER* (-ER) (KSY887/888) cells is shown. *CDC5* overexpression was induced by the addition of 400 nM Estradiol at 2 h.

(I) Kinetics of Rec8 classes in (G) was classified shown in Figure 1B. A minimum 100 cells were counted at each time point.

Figure 5. Rad61/Wpl1 plays a role in cohesin-release in late prophase-I

(A) Expression profiles of Rec8 and Rad61-Flag during meiosis were verified using *RAD61-FLAG* (KSY440/441) cells by western blotting. The protein positions are indicated with the lines on the right. Phosphorylated species of Rec8 and Rad61-Flag are shown by arrows.

(B) Bands shits of Rec8 and Rad61 were analyzed in presence and absence of 1NM-PP1 in *RAD61-FLAG* (KSY440/441) and *cdc7-as3 RAD61-FLAG* (KSY978/979) strains at the indicated time points by western blotting as shown in (A).

(C) Bands shits of Rec8 and Rad61 in *RAD61-FLAG* (KSY440/441) and *CDC5-mn RAD61-FLAG* (KSY434/435) cells were studied as shown in (A).

(D) The western blotting analysis was carried out for Rad61-Flag (Right) and Rad61-pS69, 70 (left) in *RAD61-FLAG* (KSY440/441), *rad61-S69A, S70A-FLAG* (KSY754/757) and *rad61-7A-FLAG* (KSY753/755) strains as shown in (A).

(E) Bands shits of Rec8 and Rad61 in *RAD61-FLAG* (KSY440/441) and *rec8 RAD61-FLAG* (KSY627/628) cells were analyzed as shown in (A).

(F) Localization of Rec8 (red) and Ctf19 (green) in *CDC20-mn* (KSY642/643), *CDC20-mn rad61* (KSY637/638), *CDC20-mn rad61-7A* (KSY653/654) and *CDC20-mn rec8-29A rad61-7A* (KSY1043/1044) cells. Representative image for each strain at various time points are shown.

(G) Measurement of total Rec8 and DAPI signal intensity in (F) was analyzed in Figure 1D. Error bars show the S.D. (n=3).

(H) Kinetics of Rec8-classes (F) was studied as described in Figure 1B. A minimum 100 cells were analyzed per time point. Error bars show the S.D. (n=3).

Figure 6. PLK promotes chromosome compaction in late prophase-I

(A) Representative images of *CEN4* and *TEL4* GFP foci (green) and nuclei (blue) in *CDC20-mn* (KSY991/642), *ndt80* (KSY445/467) and *CDC20-mn CDC5-mn* (KSY989/659) cells in a single focal plane of whole cell staining at each time point are shown. The bar indicates 2µm.

(B) Distances between *CEN4* and *TEL4* at each time point 0h, 5h, 8h (*CDC20-mn;* KSY991/642 and *ndt80;* KSY445/467) 10 h in *CDC20-mn CDC5-mn* (KSY989/659) were measured and plotted as a box/whisker plot. A minimum 100 nuclei were studied in each time point.

Figure 7. Meiotic prophase pathway for cleavage-independent cohesin removal. See details in the text.

Challa et al. Figure 1

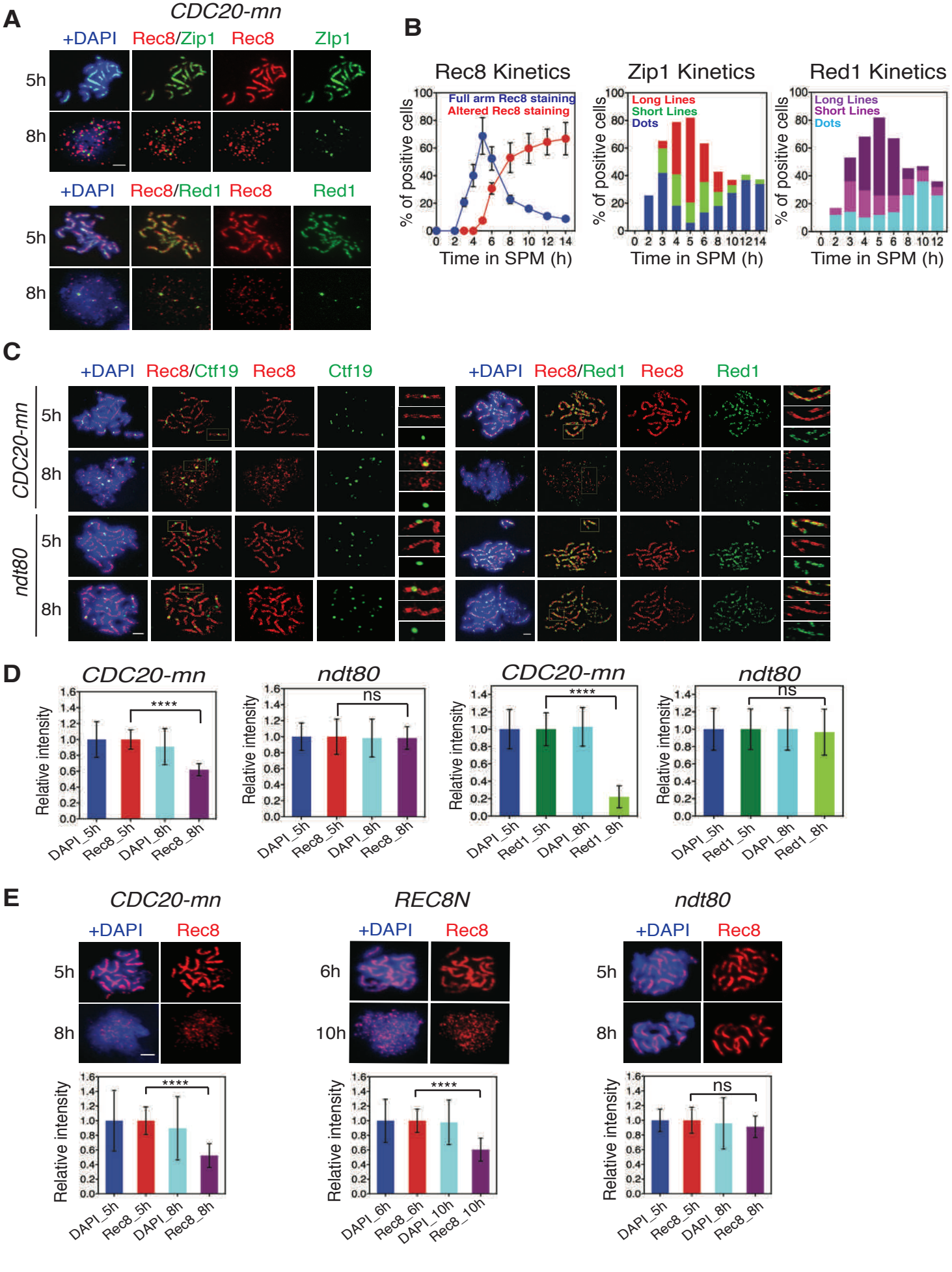

Challa et al. Figure 2

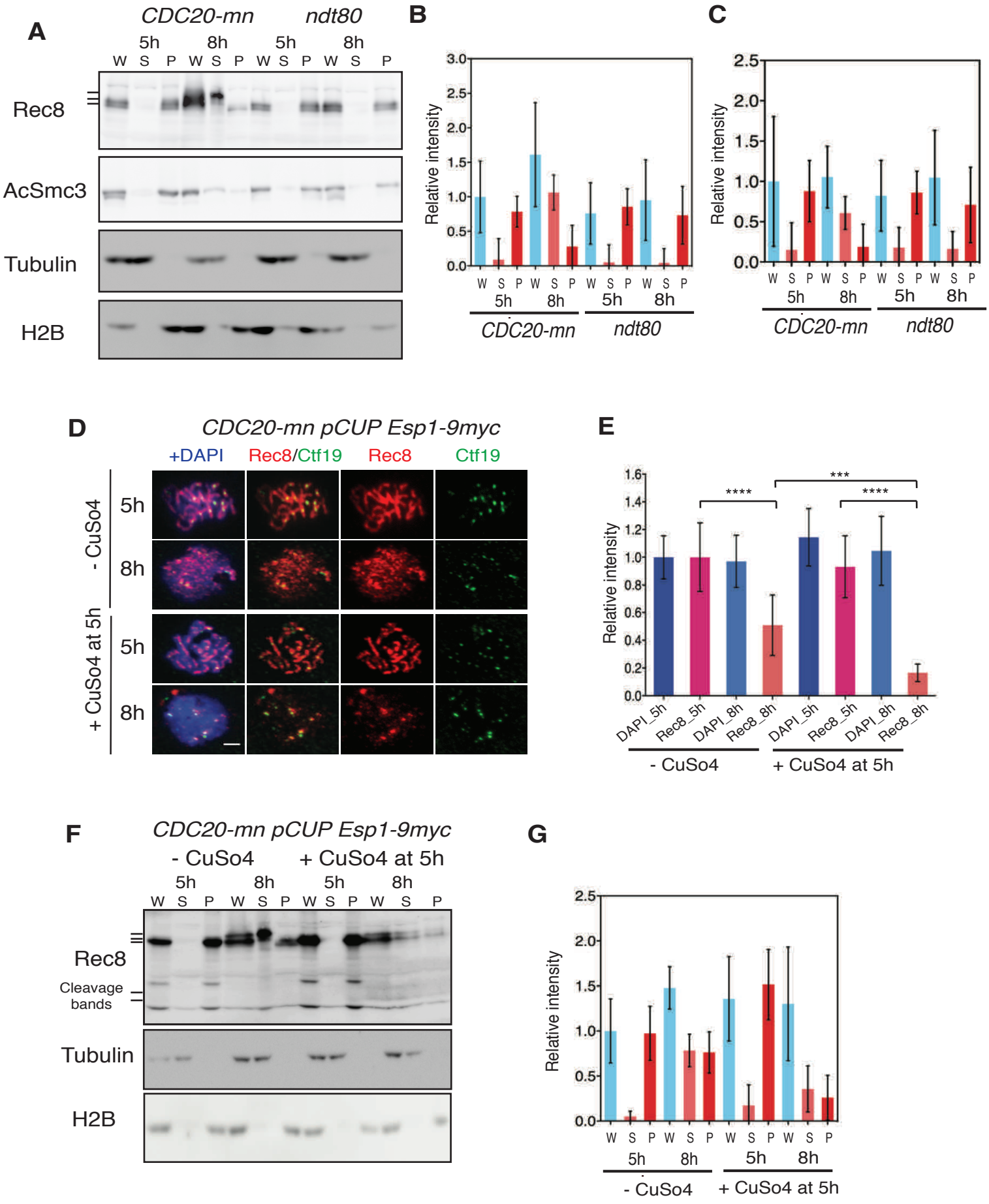

Challa et al. Figure 3

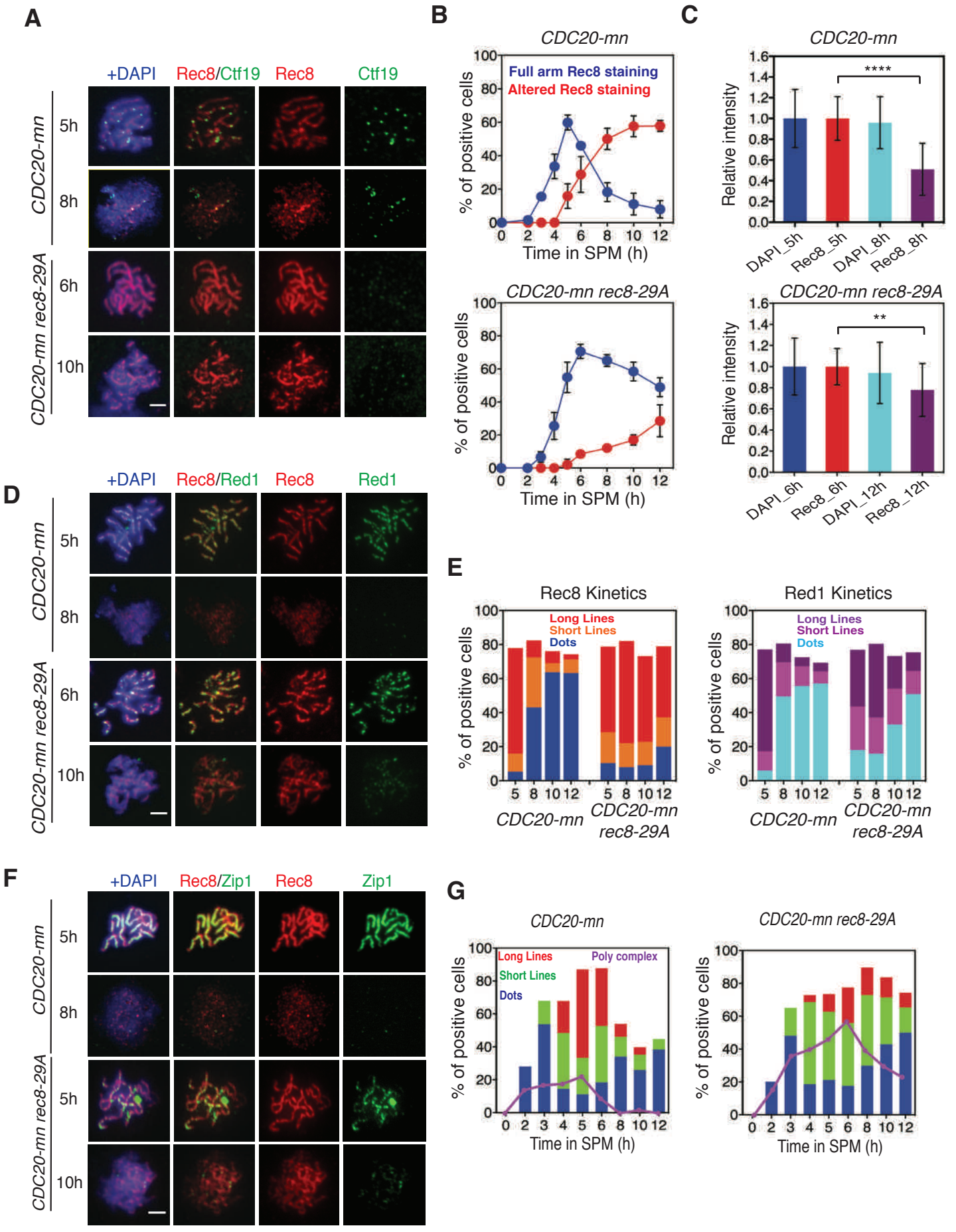

Challa et al. Figure 4

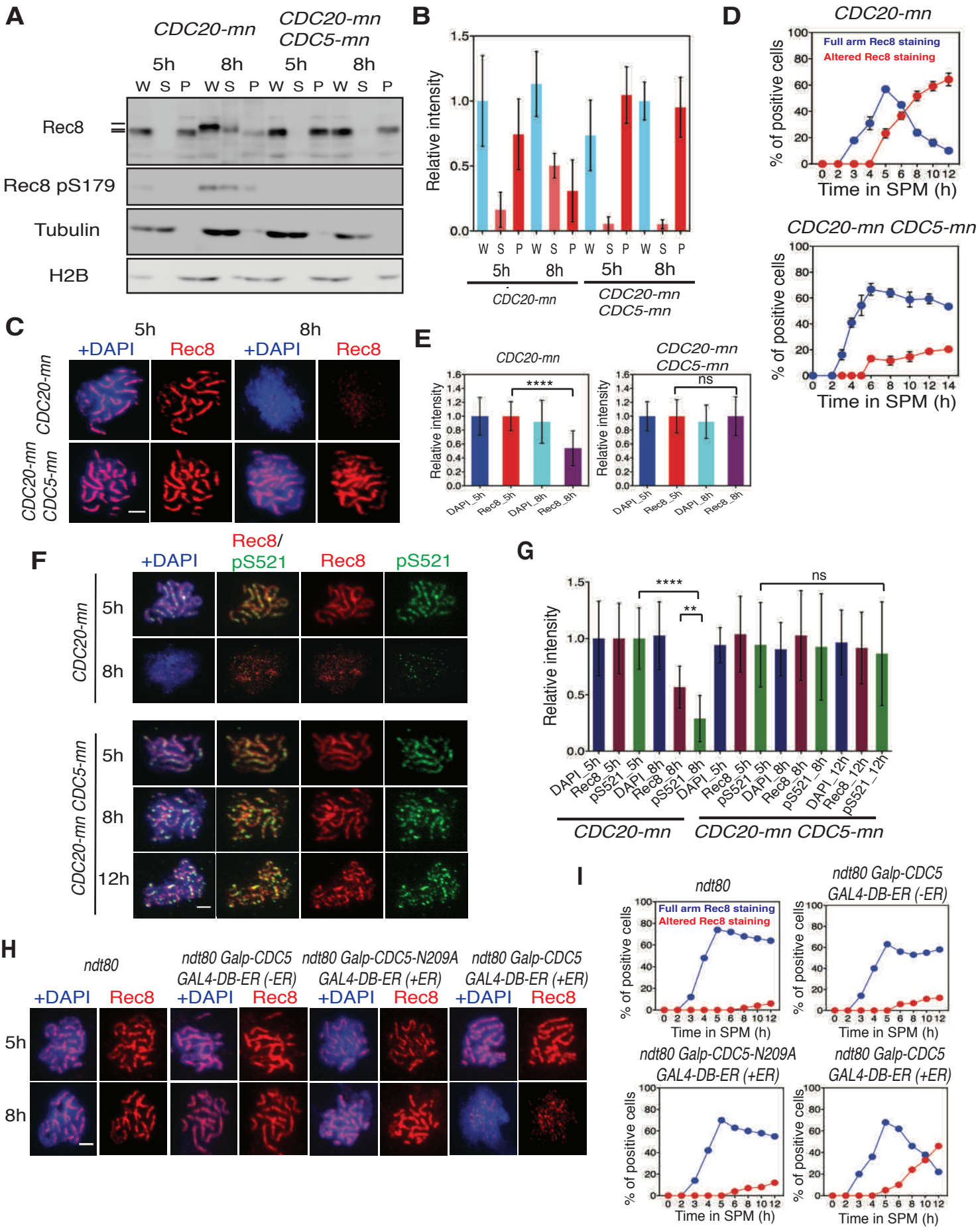

Challa et al. Figure 5

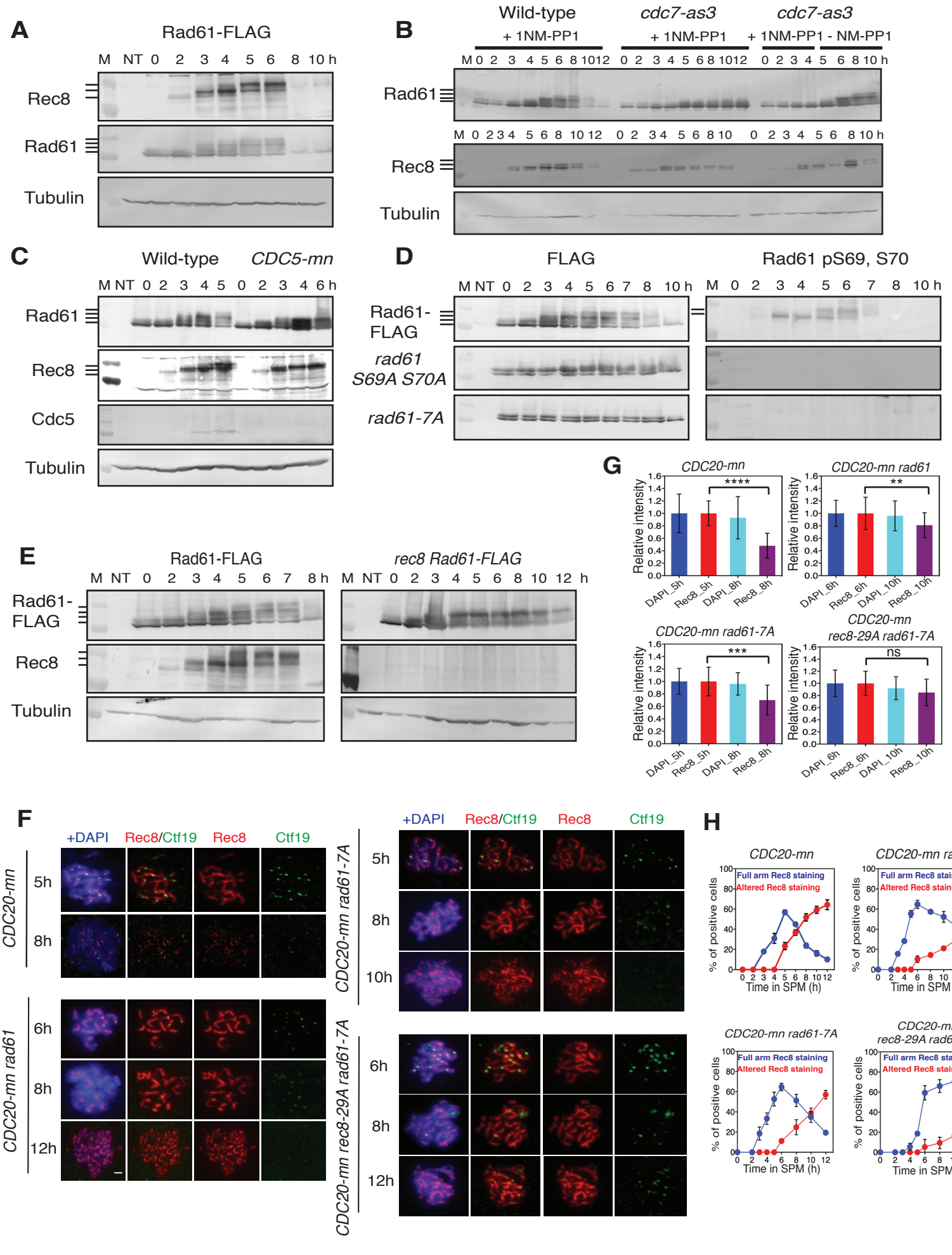

Challa et al. Figure 6

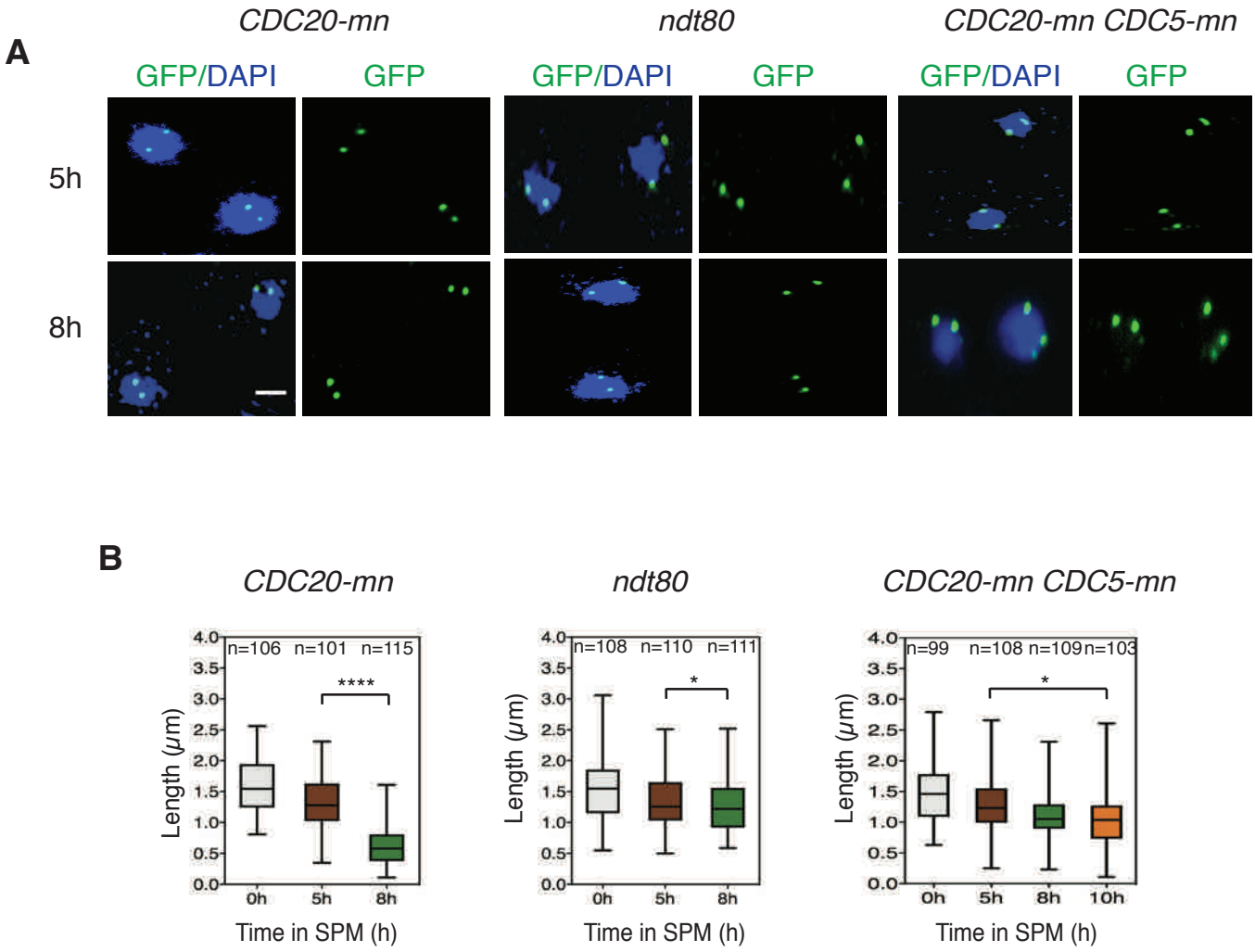

Figure 7 Challa et al.